European Radiology (2022) 32:5106–5118
https://doi.org/10.1007/s00330-022-08717-3

GASTROINTESTINAL

The application of apparent diffusion coefficients derived from intratumoral and peritumoral zones for assessing pathologic prognostic factors in rectal cancer

Yi Yuan[1] · Xiao-li Chen[2] · Zhen-lin Li[3] · Guang-wen Chen[1] · Hao Liu[4] · Yi-Sha Liu[5] · Ming-hui Pang[6] · Si-yun Liu[7] · Hong Pu[1] · Hang Li[1]

Received: 12 February 2022 / Revised: 12 February 2022 / Accepted: 5 March 2022 / Published online: 23 March 2022

Abstract

Objective To investigate the diagnostic performance of the apparent diffusion coefficient (ADC) derived from intratumoral and peritumoral zones for assessing pathologic prognostic factors in rectal cancer.

Materials and methods One hundred forty-six patients with rectal cancer who underwent preoperative MRI were prospectively enrolled. Two radiologists independently placed free-hand regions of interest (ROIs) in the largest tumor cross section and three small ROIs on the peritumoral zone adjacent to the tumor contour. Maximum values of tumor ADC (ADC_{tmax}), minimum values of tumor ADC (ADC_{tmin}), mean values of tumor ADC (ADC_{tmean}), mean values of peritumor ADC (ADC_{pmean}), and ADC_{pmean}/ADC_{tmean} (ADC ratio) were obtained on ADC maps and correlated with prognostic factors using uni- and multivariate logistic regression, and receiver operating characteristic curve (ROC) analysis.

Results Interobserver agreement was excellent for ADC_{tmax} and ADC_{tmean} (intraclass correlation coefficient [ICC], 0.915–0.958), and were good for ADC_{tmin}, ADC_{pmean}, and ADC ratio (ICC, 0.774–0.878). The ADC ratio was significantly higher in the poor differentiation, T3–4 stage, lymph node metastasis (LNM)–positive, extranodal extension (ENE)–positive, tumor deposit (TD)–positive, and lymphovascular invasion (LVI)–positive groups than that in the well–moderate differentiation, T1–2 stage, LNM-negative, ENE-negative, TD-negative, and LVI-negative groups (p = 0.008, < 0.001, < 0.001, 0.001, < 0.001, and < 0.001, respectively). The area under the ROC curve (AUC) of the ADC ratio was the highest for assessing poor differentiation (0.700), T3–4 stage (0.707), LNM-positive (0.776), TD-positive (0.848), and LVI-positive (0.778). Both the ADC ratio (AUC = 0.677) and ADC_{pmean} (AUC = 0.686) showed higher diagnostic performance for assessing ENE.

Conclusion The ADC ratio could provide better predictive performance for assessing preoperative prognostic factors in resectable rectal cancer.

Key Points

- *Both the peritumor/tumor ADC ratio and ADC_{pmean} are correlated with important prognostic factors of resectable rectal cancer.*
- *Both peritumor ADC and peritumor/tumor ADC ratio had higher diagnostic performance than tumor ADC for assessment of prognostic factors in resectable rectal cancer.*
- *Peritumor/tumor ADC ratio showed the most capability for the assessment of prognostic factors in resectable rectal cancer.*

Keywords Rectal neoplasms · Diffusion magnetic resonance imaging · Lymphatic metastasis · Extranodal extension

Abbreviations

ADC ratio	ADC_{pmean}/ADC_{tmean}
ADC_{pmean}	Mean values of peritumor ADC
ADC_{tmax}	Maximum values of tumor ADC
ADC_{tmean}	Mean values of tumor ADC
ADC_{tmin}	Minimum values of tumor ADC
AUCs	Areas under the receiver operating characteristic curves
CI	Confidence interval
ENE	Extranodal extension
ICC	Intraclass correlation coefficient
LNM	Lymph node metastasis

Hang Li and Hong Pu contributed equally to this study.

✉ Hang Li
lihang111222@126.com

Extended author information available on the last page of the article

LVI	Lymphovascular invasion
ROC	Receiver operating characteristic
ROI	Region of interest
SD	Standard deviations
TD	Tumor deposit

Introduction

Colorectal cancer has become the third most frequent malignancy in the world [1]. Its prognosis depends on different factors, such as poor differentiation, deep tumor invasion, and lymphovascular invasion (LVI) [2, 3]. Moreover, lymph node metastasis (LNM) and tumor deposits (TDs), which are both recognized as N staging elements of the 8th Tumor Node Metastasis (TNM) staging system [4], play an important role in determining the therapeutic strategy [5–7]. Extranodal extension (ENE), defined as the extension of tumor cells through the nodal capsule into the perinodal fatty tissue, is an important prognostic factor in patients with several types of malignancies [4]. Although ENE in patients with rectal cancer is not yet considered the TNM staging system, several studies have reported that ENE is an adverse prognostic factor [8–10]. Therefore, accurate preoperative assessments of these prognostic factors are important for improving the prognosis of this disease.

As a noninvasive imaging modality with no ionizing radiation and excellent soft-tissue contrast, MRI has been widely implemented for prognostic assessment of rectal cancer. The traditional morphological signs were applied to evaluate the T category, anal sphincter complex involvement, mesorectal fascia involvement, and extramural vascular invasion of rectal cancer [11]. However, defining LNM and TD remains challenging by using size criteria and morphological criteria [12, 13]. Moreover, tumor differentiation, LVI, and ENE can only be determined by the postoperative pathological examination. Diffusion-weighted imaging (DWI) is a functional technique that provides information about water mobility, tissue cellularity, and the integrity of the cellular membrane. The apparent diffusion coefficient (ADC) value is used to quantify water diffusion, which provides an estimation of tumor heterogeneity [14]. However, tumor heterogeneity is not only solely limited to cancer cells but also relates to nonmalignant and infiltrating cells surrounding the tumor, commonly referred to as the microenvironment. The role of the tumor environment is important because it is the interaction between tumor cells and the surrounding microenvironment that influences tumor evolution and progression [15]. Previous studies have confirmed that peritumoral regions surrounding tumors contain valuable information in cancer studies of breast [16], esophageal [17], and endometrial cancer [18]. Although several studies have reported associations between intratumoral ADC values and prognostic factors of rectal cancer, peritumoral ADC values have not been reported [19, 20]. Therefore, the purpose of this study was to explore the diagnostic value of the ADC value of the intratumoral and peritumoral zones for the assessment of prognostic factors in resectable rectal cancer.

Materials and methods

Study population

Our institutional review board approved this prospective study, and all study participants provided informed consent. A total of 204 consecutive patients (mean age ± SD, 62 ± 11.4 years old, with a range from 24 to 88 years) with resectable rectal cancer who underwent radical surgery between January 2017 and March 2021 were enrolled in this study. The inclusion criteria were nonmucinous rectal adenocarcinoma proven by endoscopic biopsy. The exclusion criteria were as follows: (1) tumors were not visible on MR images (n = 6); (2) insufficient image quality due to gas-induced susceptibility artifacts or movement artifacts (n = 8); (3) any contraindication for surgery (n = 2); (4) nonresectable and/or metastatic disease (n = 36); and (5) presence of mucinous tumors, which have a very low cellular density and will therefore exhibit high ADC values (n = 6).

Imaging protocol

MRI was performed using a 1.5-T scanner (MAGNETOM Aera, Siemens Healthineers) with body coils. Patients were given 20 mg of scopolamine butylbromide (Buscopan, Boehringer Ingelheim) intramuscularly 30 min before MRI to reduce bowel motion. Patients did not receive rectal distention before MR examinations. The conventional MRI protocol included sagittal, axial (perpendicular to the long axis of the rectum), oblique coronal T2-weighted images, and no fat saturation and DWI (perpendicular to the long axis of the rectum). The acquisition parameters for T2-weighted images were as follows: TR/TE, 4590/73; field of view, 220 mm^2; matrix size, 256 × 512; section thickness, 3.5 mm; and intersection gap, 0.7 mm. Axial DW images of the pelvis were obtained with the following parameters: 4600/59; number of signals acquired, eight; field of view, 360 mm^2; section thickness, 5 mm; and b values, 0 and 800 s/mm^2. ADC maps were created automatically by the device.

Image analysis

The MRI images were independently reviewed by the two radiologists (Y.Y. and H.L., 4 and 10 years of experience in reading rectal MRI) who were blinded to the patients' clinical and pathological information but were aware that the patients had been

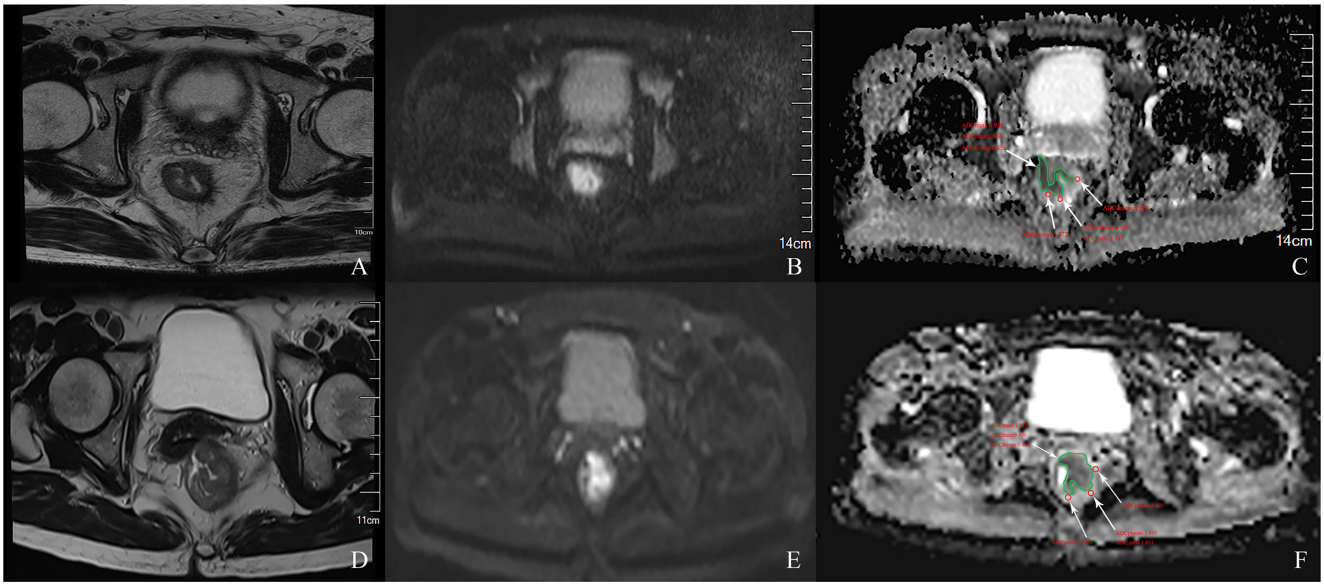

Fig. 1 Methods used to measure the tumor and peritumor apparent diffusion coefficient (ADC) values. **A**–**C** A 61-year-old man with T3N2M0, extranodal extension (ENE)–positive, tumor deposit (TD)–positive, lymphovascular invasion (LVI)–positive, and poorly differentiated rectal cancer. Regarding the tumor ADC, the slice with the largest tumor cross section was selected, and the region of interest (ROI) was placed inside the tumor that contained the largest tumor area with reference to (**A**) T2WI imaging and (**B**) DWI. ADC_{tmax}, ADC_{tmin}, and ADC_{tmean} are recorded as 0.919×10^{-3} mm^2/s, 0.668×10^{-3} mm^2/s, and 0.833×10^{-3} mm^2/s, respectively. For the peritumoral ADC, three elliptical ROIs were drawn along the tumor margin where the ADC values visually appeared to be most increased in the (**C**) peritumoral zone. The maximum mean value of the three ADC values was designated as the peritumoral ADC (ADC_{pmean}). The ADC_{pmean} and ADC ratio are 2.033×10^{-3} mm^2/s and 2.441, respectively. **D**–**F** A 65-year-old woman with T3N1M0, extranodal extension (ENE)–negative, tumor deposit (TD)–negative, lymphovascular invasion (LVI)–negative, and moderate differentiation rectal cancer. The ADC_{tmax}, ADC_{tmin}, ADC_{tmean}, ADC_{pmean}, and ADC ratio were recorded as 1.124×10^{-3} mm^2/s, 0.690×10^{-3} mm^2/s, 0.891×10^{-3} mm^2/s, 1.649×10^{-3} mm^2/s, and 1.851, respectively

diagnosed with rectal cancer. To measure the ADC of the tumor, the largest tumor cross section was selected on the ADC map. Regions of interest (ROIs) were applied to intratumoral and peritumoral zones (Fig. 1). The radiologists reviewed the T2WI and DWI images and determined the location of the tumor. According to the previous method described by Mori et al [16], three elliptical ROIs (mean area, 20 mm^2) were then drawn along the tumor margin where the ADC values visually appeared to be most increased on the peritumoral zone for measuring the ADC values of the individual ROIs: the maximum mean values of these ADC were designated as the peritumoral ADC (ADC_{pmean}). For intratumoral ADC measurements, ROIs were placed inside the tumor that contained the largest tumor area, while cystic, necrotic, and visible vascular structures were carefully avoided by referring to T2-weighted images. Maximum, minimum, and mean values of intratumoral ADC were recorded and designated as ADC_{tmax}, ADC_{tmin}, and ADC_{tmean}, respectively. The peritumor-tumor ADC ratio was calculated according to the following formula: ADC ratio= ADC_{pmean}/ADC_{tmean}.

Surgical histologic findings

All patients underwent radical total mesorectal excision, indicating that the entire mesorectal fat, including all lymph nodes, should be excised. At least 12 regional lymph nodes should be examined. A specialist with 13 years of experience in rectal pathology examined operative specimens and reported the histopathologic findings according to the College of American Pathologists guidelines. ENE was defined as cancer cells infiltrating the extranodal adipose tissue extending through or beyond the lymph node capsule according to a previous study [21]. Histology type, depth of tumor invasion, lymph node status, ENE, TD, and LVI were reported.

Statistical analysis

The statistical analyses were performed using SPSS version 22 (IBM Corporation) and MedCalc (Version 16.8). The intraclass correlation coefficients (ICCs) were calculated by a two-way mixed model with absolute agreement to evaluate the agreement between the ADC values measured by the two radiologists. Twenty-three patients were randomly selected for ICC. The ICC was classified into poor (ICC < 0.5), moderate (0.5 ≤ ICC < 0.75), good (0.75 ≤ ICC < 0.9), and excellent (ICC ≥ 0.9) [22]. The interradiologist measurements for ADC values were further compared using Bland-Altman plots to examine bias and limits of agreement [23]. The mean difference and the 95% limits of agreement (mean difference ± 1.96 standard deviations [SDs]) are illustrated. The ADC values were averaged between the two radiologists for further

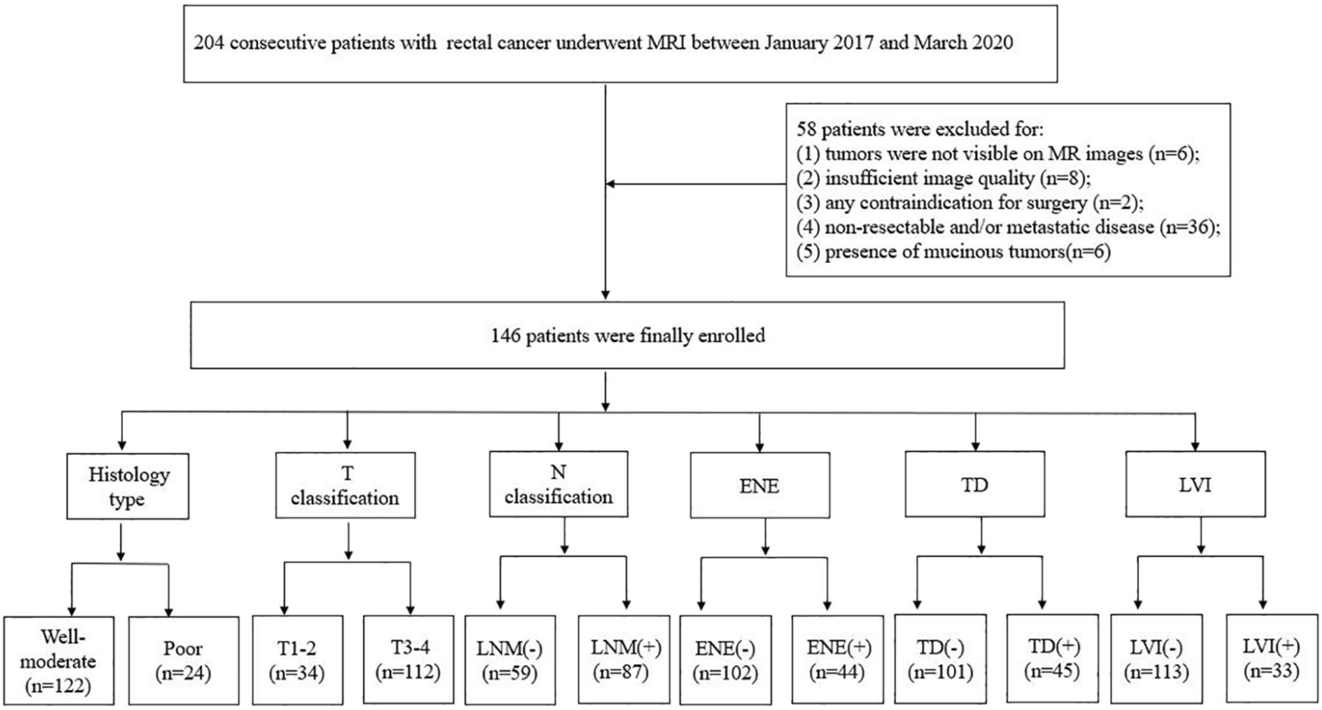

Fig. 2 Flow diagram shows the inclusion and exclusion criteria for the study

analysis. As parameters were normally distributed, Student's *t* tests and one-way ANOVA were used to compare statistical difference in different groups. As parameters were not normally distributed, Mann-Whitney *U* test and Kruskal-Wallis *H* test were used for comparisons of different groups. Univariate and multivariate logistic regression analyses were sequentially performed among ADC values to screen out the independent risk factors for tumor differentiation, T classification, LNM, ENE, TD, and LVI. The factors with a p value < 0.05 during multivariate logistic regression were determined to be independent risk factors. Optimal cutoffs for each ADC parameter were determined at points that maximized Youden's *J* index based on receiver operating characteristic (ROC) curves. Youden's index is calculated by specificity + sensitivity − 1 [24]. Two-sided $p < 0.05$ represents statistical significance among all statistics.

Results

Relationship between clinicopathologic characteristics and ADC parameters

The remaining 146 patients (mean age ± SD, 64 ± 11.6 years old; range 26–88 years) constituted the population of the current study (Fig. 2). The results of correlations between clinical characteristics and ADC parameters are shown in Table 1. The results of correlations between prognostic factors and ADC parameters are shown in Table 2 and Fig. 3. The values of ADC_{tmin} and ADC_{tmean} were larger in the T1–2 classification, LNM-negative, TD-negative, and LVI-negative groups than those in the T3–4 classification, LNM-positive, TD-positive, and LVI-positive groups, respectively ($p \leq 0.001$–0.044). However, the value of ADC_{tmin} was larger in the ENE-negative group than in the ENE-positive group ($p = 0.017$). The values of ADC_{pmean} and ADC ratio were smaller in the tumor with well–moderate differentiation, T1–2 classification, LNM-negative, ENE-negative, TD-negative, and LVI-negative groups than those in the tumor with poor differentiation, T3–4 classification, LNM-positive, ENE-positive, TD-positive, and LVI-positive groups, respectively ($p \leq 0.001$–0.011).

Univariate and multivariate analysis

The univariate and multivariate logistic regression results for screening out the independent risk factors for prognosis are summarized in Table 3. The ADC ratio was an independent risk factor for histology type (odds ratio [OR] with 95% confidence interval [CI], 7.008 [95% CI: 1.757–27.954]; $p = 0.006$). T classification, ADC_{tmin}, ADC_{pmean}, and ADC ratio were independent risk factors for predicting LNM (OR with 95% CI, 1.713 [95% CI: 1.041–2.817], 0.619 [95% CI: 0.480–0.799], 1.391 [95% CI: 1.197–1.616], and 1.290 [95%CI: 1.145–1.454]; $p = 0.030$, < 0.001, < 0.001, and < 0.001, respectively). T classification, ADC_{tmin}, ADC_{pmean}, and ADC ratio were independent risk factors for predicting ENE (OR with 95% CI, 1.780 [95% CI: 1.001–3.293], 0.689

Table 1 Relationship between clinicopathologic characteristics and ADC parameters

Parameters	Gender			Age			Location			
	Male (n = 99)	Female (n = 47)	p	< 65 (n = 70)	≥ 65 (n = 76)	p	Upper (n = 46)	Middle (n = 69)	Lower (n = 31)	p
ADC_{tmax} (× 10^{-3} mm^2/s)	1.17 (1.03–1.35)	1.06 (0.91–1.19)	0.006	1.14 (1.03–1.27)	1.10 (0.92–1.35)	0.544	1.09 (0.95–1.26)	1.11 (0.94–1.29)	1.23 (1.05–1.43)	0.120
ADC_{tmin} (× 10^{-3} mm^2/s)	0.68 (0.55–0.81)	0.69 (0.60–0.78)	0.815	0.69 (0.57–0.83)	0.68 (0.57–0.78)	0.764	0.67 ± 0.19	0.71 ± 0.21	0.70 ± 0.23	0.601
ADC_{tmean} (× 10^{-3} mm^2/s)	0.89 ± 0.16	0.87 ± 0.14	0.394	0.88 (0.78–0.99)	0.85 (0.78–0.96)	0.652	0.82 (0.76–0.94)	0.89 (0.78–0.97)	0.88 (0.82–0.97)	0.150
ADC_{pmean} (× 10^{-3} mm^2/s)	1.66 (1.47–1.90)	1.55 (1.33–1.74)	0.043	1.57 (1.35–1.76)	1.69 (1.41–1.93)	0.081	1.49 (1.31–1.74)	1.66 (1.47–1.87)	1.63 (1.38–1.95)	0.120
ADC ratio	1.92 (1.56–2.20)	1.76 (1.48–2.18)	0.391	1.80 ± 0.43	1.94 ± 0.66	0.137	1.86 ± 0.69	1.89 ± 0.52	1.83 ± 0.44	0.900

ADC, apparent diffusion coefficient; *ADC_{tmin}, ADC_{tmean}, ADC_{tmax}*, minimum, mean, and maximum values of tumor ADC, respectively; *ADC_{pmean}*, mean values of peritumor ADC; *ADC ratio*, ADC_{pmean}/ADC_{tmean}

[95% CI: 0.507–0.935], 1.246 [95% CI: 1.059–1.465], and 1.104 [95% CI: 1.000–1.220]; p = 0.04, 0.017, < 0.001, and 0.032, respectively). T classification, histological type, ADC_{pmean}, and ADC ratio were independent risk factors for predicting TD (OR with 95% CI, 2.134 [95% CI: 1.072–4.245], 6.957 [95% CI: 1.605–30.159], 1.556 [95%CI: 1.273–1.901], and 1.437 [95%CI: 1.236–1.670]; p = 0.031, 0.01, < 0.001, and < 0.001, respectively). ADC_{tmin}, ADC_{pmean}, and ADC ratio were independent risk factors for predicting LVI (OR with 95%CI, 0.686 [95%CI: 0.531–0.886], 1.313 [95%CI: 1.126–1.530], and 1.207 [95%CI: 1.072–1.360]; p = 0.004, 0.011, and 0.002, respectively).

Diagnostic performance of ADC parameters for assessment of clinicopathological characteristics

As illustrated in Table 4 and Fig. 4, the difference in AUC between the ADC ratio and ADC_{pmean} was not significant in distinguishing tumor differentiation (AUC, 0.700 vs. 0.664, p = 0.336). The AUCs of 0.707, 0.663, 0.622, and 0.614 for the ADC ratio, ADC_{pmean}, ADC_{tmean}, and ADC_{tmin} were not significantly different from each other in distinguishing T classification (p = 0.098–0.586). The AUC was greater for the ADC ratio than for the ADC_{tmean} (0.776 vs. 0.621, p = 0.001) for predicting LNM. However, the AUC for ADC ratio was not significantly greater than either ADC_{tmin} (0.776 vs. 0.697, p = 0.115) or ADC_{pmean} (0.776 vs. 0.748, p = 0.320) for predicting LNM. The AUCs of 0.686, 0.677, and 0.625 for ADC_{pmean}, ADC ratio, and ADC_{tmin} were not significantly different from each other for assessing ENE (p = 0.420–0.782). For predicting TD and LVI, the AUC for ADC ratio was significantly better compared with either ADC_{tmin} (0.848 vs. 0.635, p < 0.001; 0.778 vs. 0.656, p = 0.004, respectively) or ADC_{tmean} (0.848 vs. 0.682, p < 0.001; 0.778 vs. 0.636, p = 0.002, respectively), but there were no significant differences between ADC ratio and ADC_{pmean} (0.848 vs. 0.819, p = 0.362; 0.778 vs. 0.735, p = 0.245, respectively).

Interobserver agreement of ADC parameters

Interobserver agreement was excellent for ADC_{tmax} (intraclass correlation coefficient [ICC], 0.915; 95% CI, 0.811–0.963) and ADC_{tmean} (ICC, 0.958; 95% CI, 0.903–0.982). Interobserver agreement was good for ADC_{tmin} (ICC, 0.844; 95% CI, 0.668–0.931), ADC_{pmean} (ICC, 0.774; 95% CI, 0.538–0.898), and ADC ratio (ICC, 0.878; 95% CI, 0.713–0.948).

The Bland-Altman plots representing the relationship between the differences and mean ADC values determined by the two radiologists are illustrated in Fig. 5. For ADC_{tmin}, the mean difference and 95% limits of agreement were 0.02 mm^2/

Table 2 Relationship between prognostic factors and ADC parameters

Parameters	Histology type		p	pT classification		p	LNM		p
	Well–moderate (n = 122)	Poor (n = 24)		T1–2 (n = 34)	T3–4 (n = 112)		Negative (n = 59)	Positive (n = 87)	
ADC_{tmax} (× 10^{-3} mm^2/s)	1.13 (0.98–1.30)	1.18 (0.94–1.32)	0.792	1.14 (0.99–1.30)	1.14 (0.97–1.31)	0.806	1.14 (1.00–1.36)	1.13 (0.95–1.27)	0.638
ADC_{tmin} (× 10^{-3} mm^2/s)	0.69 (0.59–0.80)	0.64 (0.53–0.75)	0.083	0.76 (0.64–0.84)	0.68 (0.55–0.78)	0.044	0.78 ± 0.23	0.63 ± 0.17	< 0.001
ADC_{tmean} (× 10^{-3} mm^2/s)	0.89 ± 0.14	0.83 ± 0.19	0.109	0.91 (0.81–1.03)	0.84 (0.76–0.96)	0.032	0.88 (0.81–1.01)	0.83 (0.76–0.96)	0.013
ADC_{pmean} (× 10^{-3} mm^2/s)	1.61 (1.35–1.80)	1.84 (1.47–2.05)	0.011	1.54 (1.17–1.68)	1.66 (1.42–1.90)	0.004	1.49 (1.26–1.66)	1.73 (1.50–1.97)	< 0.001
ADC ratio	1.79 ± 0.45	2.28 ± 0.82	0.008	1.57 (1.24–1.98)	1.97 (1.60–2.28)	< 0.001	1.63 (1.31–1.93)	2.08 (1.70–2.39)	< 0.001

Parameters	ENE		p	TD		p	LVI		p
	Negative (n = 102)	Positive (n = 44)		Negative (n = 101)	Positive (n = 45)		Negative (n = 113)	Positive (n = 33)	
ADC_{tmax} (× 10^{-3} mm^2/s)	1.14 (0.98–1.29)	1.13 (0.95–1.33)	0.878	1.14 (1.00–1.37)	1.09 (0.92–1.27)	0.193	1.14 (1.00–1.32)	1.08 (0.92–1.30)	0.597
ADC_{tmin} (× 10^{-3} mm^2/s)	0.71 (0.59–0.83)	0.65 (0.54–0.76)	0.017	0.73 (0.60–0.83)	0.67 (0.54–0.74)	0.009	0.72 (0.60–0.82)	0.63 (0.53–0.72)	0.006
ADC_{tmean} (× 10^{-3} mm^2/s)	0.87 (0.78–1.00)	0.83 (0.78–0.95)	0.230	0.89 (0.81–1.00)	0.80 (0.75–0.89)	< 0.001	0.87 (0.79–0.98)	0.82 (0.72–0.90)	0.017
ADC_{pmean} (× 10^{-3} mm^2/s)	1.53 ± 0.37	1.75 ± 0.29	< 0.001	1.48 ± 0.36	1.84 ± 0.21	< 0.001	1.56 (1.33–1.77)	1.85 (1.68–2.02)	< 0.001
ADC ratio	1.71 (1.40–2.12)	2.07 (1.82–2.40)	0.001	1.68 (1.37–2.03)	2.21 (2.01–2.54)	< 0.001	1.72 (1.45–2.07)	2.26 (1.99–2.48)	< 0.001

Note: *ADC*, apparent diffusion coefficient; ADC_{tmin}, ADC_{tmean}, ADC_{tmax}, minimum, mean, and maximum values of tumor ADC, respectively; ADC_{pmean}, mean values of peritumor ADC; *ADC ratio*, ADC_{pmean}/ADC_{tmean}; *LNM*, lymph node metastasis; *ENE*, extranodal extension; *TD*, tumor deposit; *LVI*, lymphovascular invasion s and −0.18 to +0.23 mm²/s, respectively; for ADC_{tmax}, the mean difference and 95% limits of agreement were −0.02 mm^2/s and −0.28 to +0.24 mm^2/s, respectively; for ADC_{tmean}, the mean difference and 95% limits of agreement were −0.01 mm^2/s and −0.1 to +0.08 mm^2/s, respectively; for ADC_{pmean}, the mean difference and 95% limits of agreement were 0.00 mm^2/s and −0.37 to +0.37 mm^2/s, respectively; for ADC ratio, the mean difference and 95% limits of agreement were 0.03 and −0.19 to +0.25, respectively. Overall, there was good agreement for all ADC values measured by the two radiologists, and the majority of points fell within the 95% limits of agreement range.

Discussion

In this study, we evaluated the diagnostic performance of ADC parameters derived from the intratumoral and peritumoral zones for assessing prognostic factors in resectable rectal cancer. Our study demonstrated that the ADC value of the peritumoral zone, especially the peritumor-tumor ADC ratio, could be potentially useful for evaluating prognostic factors. However, the ADC values of the tumor were not reliable enough.

A previous study addressed the diagnostic performance of tumor ADC for assessing prognostic factors in rectal cancer and indicated conflicting results. Li et al reported that the maximum ADC value obtained with several small ROIs could not differentiate the histologic type, but it provided valuable diagnostic performance for assessing the LVI and N stage [20]. Our study indicated that the maximum ADC value obtained by drawing the largest tumor area ROI could not be used to assess prognostic factors. Possible reasons for these inconsistent outcomes included the different ROI delineations and large sample size in our study. Liu et al showed that the ADC_{tmean} and ADC_{tmin} obtained by drawing the whole tumor ROIs could differentiate histological grade [19]. Curvo-Semedo et al also found that the ADC_{tmean} obtained by selecting smaller round/oval-shaped ROIs could differentiate histological type [25]. However, Sun et al reported that the ADC_{tmean} value obtained by drawing three ROIs as large as possible could not be used to differentiate histology type [26]. Our study showed that the ADC_{tmean} and ADC_{tmin} values could not differentiate histology type. The explanation of these different outcomes could be that we combined well differentiation and moderate differentiation as well–moderate differentiation for statistical analysis because of the small sample size for well differentiation. Moreover, the different methods of ROI delineation and the choice of different *b* values may result in these differences. Regarding the assessment of the other prognostic factors, both the ADC_{tmean} and ADC_{tmin} values could assess T classification, LNM, and extramural vascular invasion but with lower diagnostic performance [19]. Our results also indicated that ADC_{tmean} and

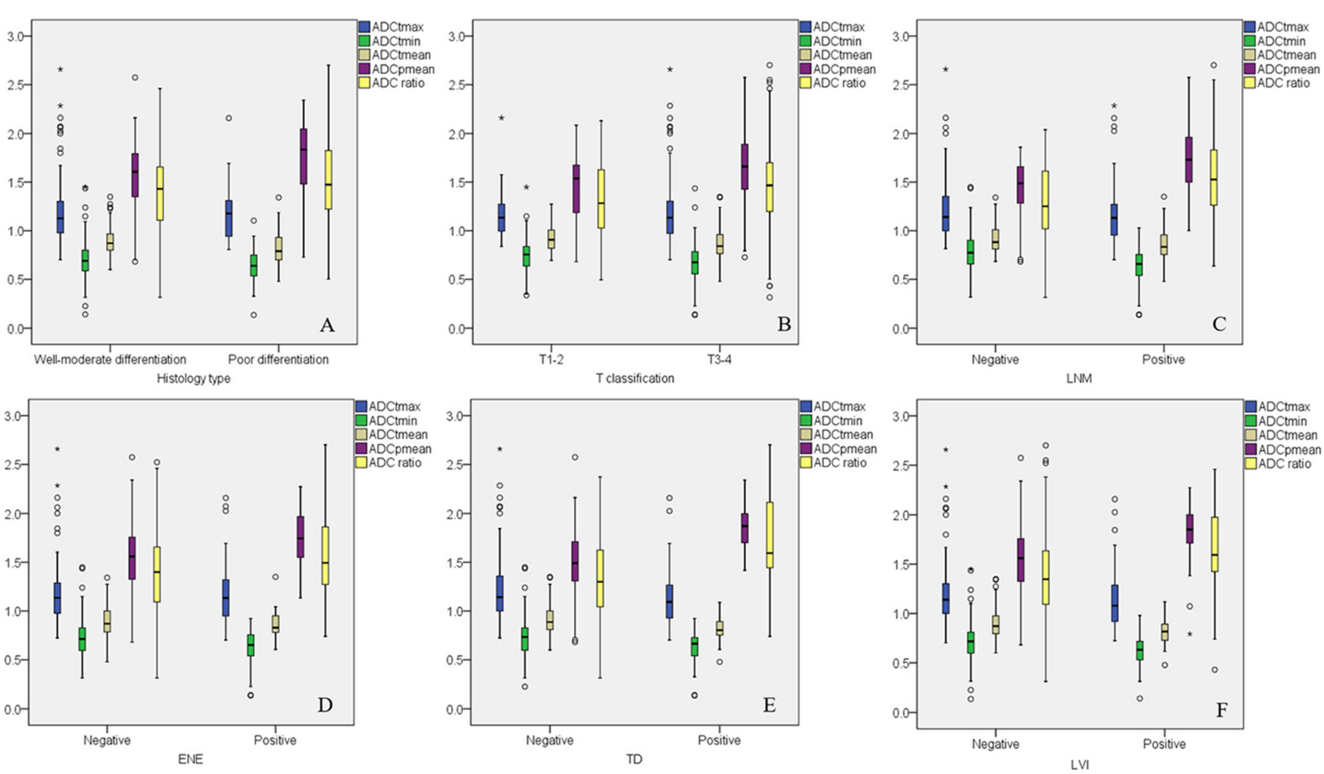

Fig. 3 Box plots show the association of ADC_{tmax}, ADC_{tmin}, ADC_{tmean}, ADC_{pmean}, and ADC ratio with prognostic factors in rectal cancer

Table 3 Univariate and multivariate analyses of risk factors for prognostic factors

Risk factor	Univariate analysis		Multivariate analysis	
	Odds ratio	*p*	Odds ratio	*p*
Histology type				
T classification	3.911 (0.870, 17.576)	0.075		
LNM	2.304 (0.856, 6.207)	0.099		
ADC_{tmax} (× 10^{-3} mm^2/s)	0.947 (0.246, 3.645)	0.937		
ADC_{tmin} (× 10^{-3} mm^2/s)	0.998 (0.996, 1.000)	0.078		
ADC_{tmean} (× 10^{-3} mm^2/s)	0.997 (0.994, 1.000)	0.051		
ADC_{pmean} (× 10^{-3} mm^2/s)	1.002 (1.000, 1.003)	0.015	0.999 (0.997, 1.002)	0.502
ADC ratio	5.274 (2.094, 13.286)	< 0.001	7.008 (1.757, 27.954)	0.006*
T classification				
Histology type	3.911 (0.870, 17.576)	0.075		
LNM	3.716 (1.660, 8.321)	0.001	2.169 (0.860, 5.472)	0.101
ADC_{tmax} (× 10^{-3} mm^2/s)	1.214 (0.364, 4.052)	0.753		
ADC_{tmin} (× 10^{-3} mm^2/s)	0.998 (0.996, 1.000)	0.036	1.000 (0.998, 1.002)	0.964
ADC_{tmean} (× 10^{-3} mm^2/s)	0.997 (0.995, 1.000)	0.022	1.002 (0.994, 1.011)	0.552
ADC_{pmean} (× 10^{-3} mm^2/s)	5.699 (1.861, 17.449)	0.002	0.998 (0.993, 1.003)	0.484
ADC ratio	4.885 (2.051, 11.635)	< 0.001	1.029 (0.981, 1.080)	0.240
LNM				
Histology type	2.304 (0.856, 6.207)	0.099		
T classification	3.716 (1.660, 8.321)	0.001	1.713 (1.041, 2.817)	0.030*
ADC_{tmax} (× 10^{-3} mm^2/s)	0.623 (0.228, 1.698)	0.355		
ADC_{tmin} (× 10^{-3} mm^2/s)	0.996 (0.994, 0.998)	< 0.001	0.619 (0.480, 0.799)	< 0.001*
ADC_{tmean} (× 10^{-3} mm^2/s)	0.997 (0.995, 0.999)	0.008	1.009 (0.999, 1.019)	0.089
ADC_{pmean} (× 10^{-3} mm^2/s)	1.003 (1.002, 1.004)	< 0.001	1.391 (1.197, 1.616)	< 0.001*
ADC ratio	1.024 (1.015, 1.034)	< 0.001	1.290(1.145, 1.454)	< 0.001*
ENE				
Histology type	1.849 (0.749, 4.560)	0.182		
T classification	3.099 (1.111, 8.641)	0.031	1.780 (1.001, 3.293)	0.040*
ADC_{tmax} (× 10^{-3} mm^2/s)	1.076 (0.369, 3.138)	0.893		
ADC_{tmin} (× 10^{-3} mm^2/s)	0.997 (0.995, 0.999)	0.006	0.689 (0.507, 0.935)	0.017*
ADC_{tmean} (× 10^{-3} mm^2/s)	0.998 (0.996, 1.001)	0.179		
ADC_{pmean} (× 10^{-3} mm^2/s)	1.002 (1.001, 1.003)	0.001	1.246 (1.059, 1.465)	< 0.001*
ADC ratio	2.909 (1.432, 5.909)	0.003	1.104 (1.000, 1.220)	0.032*
TD				
Histology type	8.153 (3.072, 21.639)	< 0.001	6.957 (1.605, 30.159)	0.010*
T classification	2.075 (1.272, 3.386)	0.003	2.134 (1.072, 4.245)	0.031*
ADC_{tmax} (× 10^{-3} mm^2/s)	0.427 (0.127, 1.438)	0.170		
ADC_{tmin} (× 10^{-3} mm^2/s)	0.064 (0.009, 0.453)	0.124		
ADC_{tmean} (× 10^{-3} mm^2/s)	0.995 (0.992, 0.998)	0.001	1.005(0.990, 1.020)	0.495
ADC_{pmean} (× 10^{-3} mm^2/s)	1.004 (1003, 1.006)	< 0.001	1.556 (1.273, 1.901)	< 0.001*
ADC ratio	1.037 (1.023, 1.051)	< 0.001	1.437 (1.236, 1.670)	< 0.001*
LVI				
Histology type	4.810 (1.901, 12.166)	0.001	2.614 (0.842, 8.110)	0.096
T classification	1.773 (1.046, 3.007)	0.034	1.648 (0.873, 3.111)	0.124
ADC_{tmax} (× 10^{-3} mm^2/s)	0.865 (0.258, 2.899)	0.814		
ADC_{tmin} (× 10^{-3} mm^2/s)	0.997 (0.995, 0.999)	0.010	0.686 (0.531–0.886)	0.004*
ADC_{tmean} (× 10^{-3} mm^2/s)	0.996 (0.993, 0.999)	0.012	1.002 (0.991, 1.013)	0.929
ADC_{pmean} (× 10^{-3} mm^2/s)	1.002 (1.001, 1.004)	0.001	1.313 (1.126–1.530)	0.011*
ADC ratio	6.159 (2.491, 15.232)	< 0.001	1.207 (1.072–1.360)	0.002*

Note: *ADC*, apparent diffusion coefficient; ADC_{tmin}, ADC_{tmean}, ADC_{tmax}, minimum, mean, and maximum values of tumor ADC, respectively; ADC_{pmean}, mean values of peritumor ADC; *ADC ratio*, ADC_{pmean}/ADC_{tmean}; *LNM*, lymph node metastasis; *ENE*, extranodal extension; *TD*, tumor deposit; *LVI*, lymphovascular invasion. *Data are statistically significant results from logistic regression analysis

ADC_{tmin} could assess T classification, LNM, ENE, TD, and LVI, although the diagnostic performance was low. Therefore, these conflicting results and the lower diagnostic performance may indicate that the ADC value derived from the intratumoral zone is not sufficient for improving the diagnostic accuracy.

A previous study reported that the heterogeneity of the peritumoral environment has its own spatial and temporal hierarchical order, which can interact with the tumor to modulate signaling pathways and growth. Thus, it has emerged as a promising field for improving diagnosis and treatment. They concluded that extramural venous invasion scores obtained on imaging were positively correlated with heterogeneity in the peritumoral tissue of rectal cancer [27]. Chen et al also reported that the combination of tumor and peritumoral US radiomics may provide a more comprehensive understanding of tumor invasion of rectal cancer [28]. In this study, we evaluated the associations of the ADC value for peritumoral areas and the peritumor/tumor ADC ratio with prognostic factors. We found that a higher peritumor/tumor ADC ratio and ADC_{pmean} were associated with a higher tumor differentiation grade, higher T classification, and the presence of LNM, ENE, TD, and LVI. A previous study in breast cancer reported tumors with higher histological grades, and more metastatic lymph nodes are known to be associated with peritumoral edema caused by LVI [29, 30]. Our study indicated that both peritumor ADC values and peritumor/tumor ADC ratios were independent risk factors for assessing LVI. Therefore, we may presume that the presence of peritumoral edema would cause higher peritumor ADC values and result in a higher peritumor/tumor ADC ratio. We further found that ADC_{pmean} and peritumor/tumor ADC ratio had higher diagnostic performance than ADC values alone from the tumor for assessing prognostic factors. Most importantly, the peritumor/tumor ADC ratio indicated higher interobserver agreement than ADC_{pmean} and showed even better diagnostic ability to assess prognostic factors, although there were no significant differences for the AUC. The explanation could be that lower tumor ADC and higher peritumoral ADC, unsurprisingly, led to higher peritumor-tumor ADC ratios in the poor differentiation, T3–4 classification, LNM-positive, ENE-positive, TD-positive, and LVI-positive groups than well–moderate differentiation, T1–2

Table 4 Diagnostic performance for ADC parameters in discrimination of clinicopathologic characteristics of rectal cancer

Parameters	AUC	Cutoff value	Sensitivity (%)	Specificity (%)
Well–moderate vs. poor differentiation				
ADC_{pmean} ($\times 10^{-3}$ mm^2/s)	0.664	1.717	62.5	65.6
ADC ratio	0.700	2.050	66.7	68
T1–2 vs. T3–4				
ADC_{tmin} ($\times 10^{-3}$ mm^2/s)	0.614	0.684	58.8	53.7
ADC_{tmean} ($\times 10^{-3}$ mm^2/s)	0.622	0.855	61.8	51.8
ADC_{pmean} ($\times 10^{-3}$ mm^2/s)	0.663	1.563	63.4	64.7
ADC ratio	0.707	1.647	72.3	61.8
LNM (−) vs. (+)				
ADC_{tmin} ($\times 10^{-3}$ mm^2/s)	0.697	0.686	64.4	60.9
ADC_{tmean} ($\times 10^{-3}$ mm^2/s)	0.621	0.849	62.7	55.2
ADC_{pmean} ($\times 10^{-3}$ mm^2/s)	0.748	1.567	70.1	62.7
ADC ratio	0.776	1.838	70.1	72.9
ENE (−) vs. (+)				
ADC_{tmin} ($\times 10^{-3}$ mm^2/s)	0.625	0.671	58.8	59.1
ADC_{pmean} ($\times 10^{-3}$ mm^2/s)	0.686	1.637	65.9	58.8
ADC ratio	0.677	1.977	65.9	65.7
TD (−) vs. (+)				
ADC_{tmin} ($\times 10^{-3}$ mm^2/s)	0.635	0.669	61.4	62.2
ADC_{tmean} ($\times 10^{-3}$ mm^2/s)	0.682	0.840	63.4	66.7
ADC_{pmean} ($\times 10^{-3}$ mm^2/s)	0.819	1.666	77.8	70.3
ADC ratio	0.848	1.961	80	72.3
LVI (−) vs. (+)				
ADC_{tmin} ($\times 10^{-3}$ mm^2/s)	0.656	0.647	66.4	54.5
ADC_{tmean} ($\times 10^{-3}$ mm^2/s)	0.636	0.827	61.9	57.6
ADC_{pmean} ($\times 10^{-3}$ mm^2/s)	0.735	1.712	75.8	70.8
ADC ratio	0.778	2.050	75.8	73.5

Note: *ADC*, apparent diffusion coefficient; ADC_{tmin}, ADC_{tmean}, ADC_{tmax}, minimum, mean, and maximum values of tumor ADC, respectively; ADC_{pmean}, mean values of peritumor ADC; *ADC ratio*, ADC_{pmean}/ADC_{tmean}; *LNM*, lymph node metastasis; *ENE*, extranodal extension; *TD*, tumor deposit; *LVI*, lymphovascular invasion

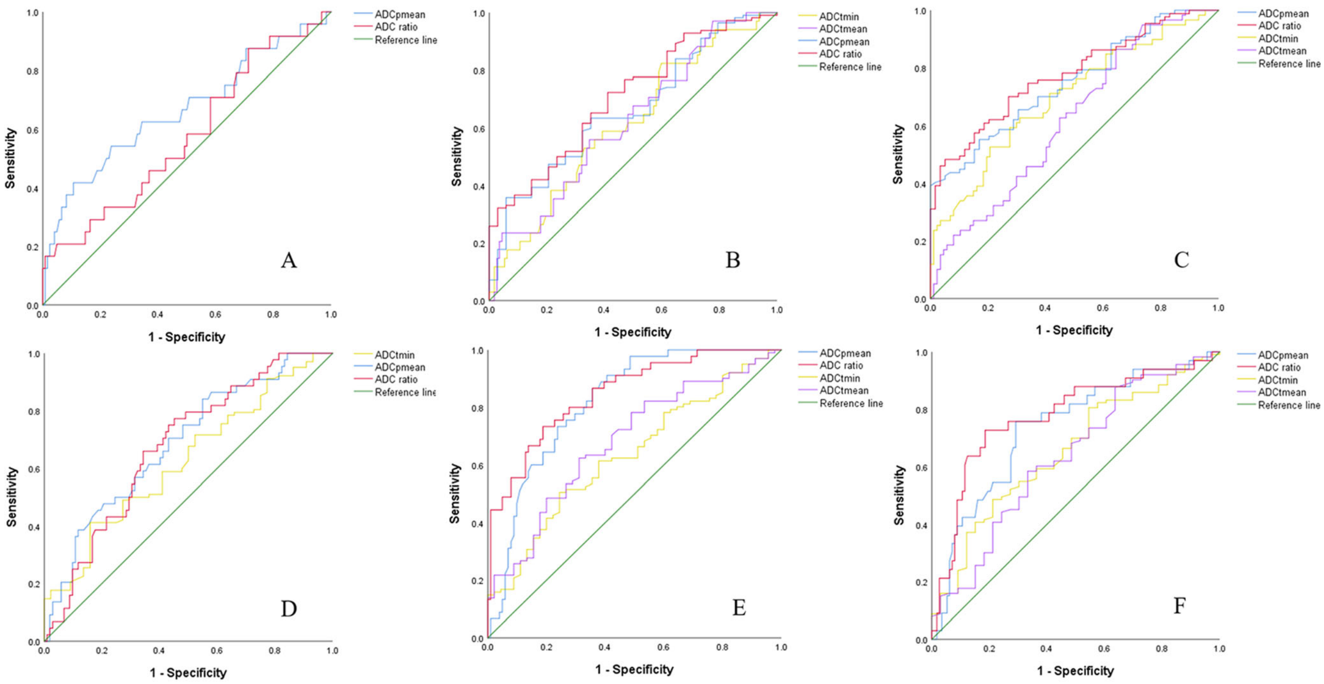

Fig. 4 Receiver operating characteristic curves. **A** Differentiation of well–moderate from poor differentiation with ADC_{pmean} (blue line) and ADC_{pmean}/ADC_{tmean} (ADC ratio) (red line). **B** Differentiation of T1–2 from T3–4 with minimum values of tumor ADC (ADC_{tmin}) (yellow line), ADC_{tmean} (purple line), ADC_{pmean} (blue line), and ADC ratio (red line). **C** Differentiation of lymph node metastasis (LNM)-negative from LNM-positive with ADC_{tmin} (yellow line), ADC_{tmean} (purple line), ADC_{pmean} (blue line), and ADC ratio (red line). **D** Differentiation of extranodal extension (ENE)–negative from ENE-positive with ADC_{tmin} (yellow line), ADC_{pmean} (blue line), and ADC ratio (red line). **E** Differentiation of tumor deposit (TD)–negative from TD-positive with ADC_{tmin} (yellow line), ADC_{tmean} (purple line), ADC_{pmean} (blue line), and ADC ratio (red line). **F** Differentiation of lymphovascular invasion (LVI)–negative from LVI-positive with ADC_{tmin} (yellow line), ADC_{tmean} (purple line), ADC_{pmean} (blue line) and ADC ratio (red line)

classification, LNM-negative, ENE-egative, TD-negative, and LVI-negative groups.

To our knowledge, no relationship between peritumor-related ADC values and prognostic factors has been reported in rectal cancer. ADC is a theoretically absolute value and can be confounded by several factors, such as different field strengths or manufacturers of the MRI scanners used, *b*-values, and ROI size [31]. The peritumor/tumor ADC ratio, which is a relative value of ADC_{pmean} and ADC_{tmean}, is more reliable and generally more applicable than the ADC value alone measured on the tumor or peritumoral area. Moreover, a previous study reported that only three small ROIs obtained by the visual assessment ROI method were sufficient to identify the needed values in breast cancer [32]. Therefore, to minimize the effects of these factors that confound DWI, three small ROIs were drawn on the peritumoral area where the ADC value appeared to be most increased adjacent to the tumor border. Nevertheless, further studies are needed to ensure the utility of the peritumor/tumor ADC ratio in the assessment of prognostic factors in different MRI systems or *b*-values and ROI sizes.

Our study has several limitations. First, we combined well differentiated and moderately differentiated tumors because there were only 5 patients with well differentiated tumors. Therefore, a much larger sample size is needed to evaluate histological type in rectal cancer. Second, this is a single-institution study without a validation cohort, and whether our results can be confirmed in other medical institutions must be assessed in future studies. Third, ADC values were obtained by the single slice ROIs that contained the largest tumor area, which might be not representative of the overall tumor profile. However, considering the measurement time, reproducibility, and diagnostic ability, the single slice ROI method is potentially useful for clinical practice. Finally, the prognostic significance of peritumor ADC values should be investigated in prospective studies with much larger cohorts, which is beyond the scope of this study.

In conclusion, ADC values derived from intratumoral and peritumoral zones could be used to assess preoperative prognostic factors in resectable rectal cancer. Among all kinds of ADC parameters, the ADC ratio could properly provide better predictive performance.

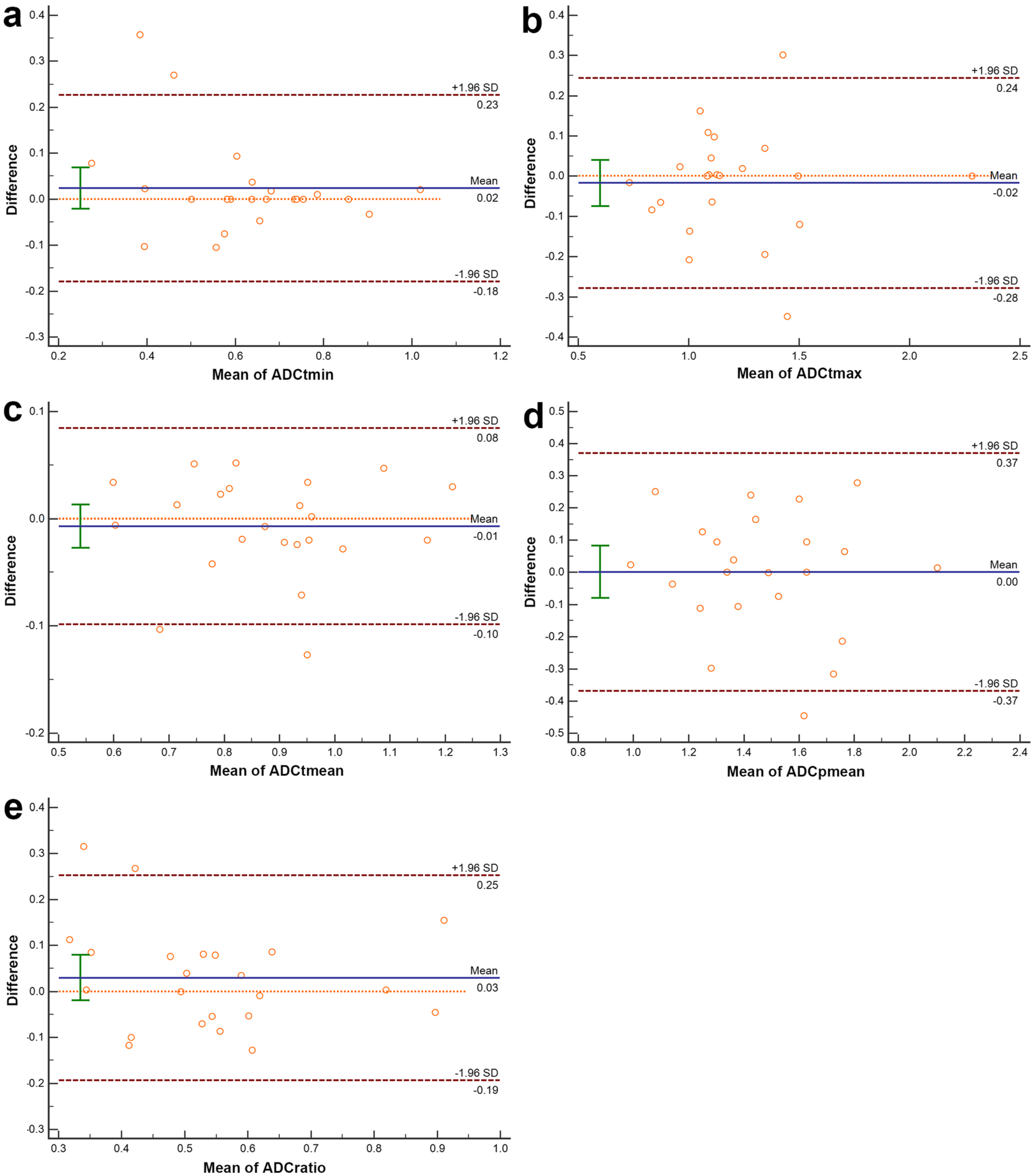

Fig. 5 Bland-Altman plots of interobserver agreement for different ADC measurements. Bland-Altman plots of ADC_{tmin} (**a**), ADC_{tmax} (**b**), ADC_{tmean} (**c**), ADC_{pmean} (**d**), and ADC ratio (**e**). The difference (*y*-axis) between the two observers is plotted against the mean value (*x*-axis) of the two radiologists' measurements. The solid horizontal blue line indicates the mean difference. The upper and lower dashed lines correspond to upper and lower 95% limits of agreement, which are calculated as the mean ± 1.96 standard deviation (SD)

Acknowledgements The authors acknowledge Siyun Liu from General Electric Healthcare and Zhenlin Li from The West China Hospital for their great support for the statistical analysis. This study was approved by the Sichuan Provincial People's Hospital institutional review board. Approval from our institutional animal care committee was not applicable because this is a human research.

Funding This study has received funding from Sichuan Science and Technology Program (grant number, 2020YFH0166) and the Key Research Project of Sichuan Province (grant number, 2022YFS0249).

Declarations

Guarantor The scientific guarantor of this publication is Hang Li.

Conflict of interest The authors of this manuscript declare that Siyun Liu is a statistician from GE Healthcare and controls of the study data. The other authors declare no competing interests.

Statistics and biometry Siyun Liu and Zhenlin Li kindly provided statistical advice for this manuscript.

Informed consent Written informed consent was obtained from all subjects (patients) in this study.

Ethical approval Institutional Review Board approval was obtained.

Methodology
• prospective
• diagnostic or prognostic study
• performed at one institution

References

1. Siegel RL, Miller KD, Jemal A (2020) Cancer statistics, 2020. CA Cancer J Clin 70:7–30
2. Koukourakis MI, Giatromanolaki A, Sivridis E, Gatter KC, Harris AL, Tumour and Angiogenesis Research Group (2005) Inclusion of vasculature-related variables in the Dukes staging system of colon cancer. Clin Cancer Res 11:8653–8660
3. Bown EJ, Lloyd GM, Boyle KM, Miller AS (2014) Rectal cancer: prognostic indicators of long-term outcome in patients considered for surgery. Int J Colorectal 29:147–155
4. Amin MB, Edge SB, Greene FL, Byrd DR, Brookland RK (2017) AJCC cancer staging manual, 8th edn. New York, NY: Springer.
5. Glynne-Jones R, Wyrwicz L, Tiret E et al (2017) Rectal cancer: ESMO Clinical Practice Guidelines for diagnosis, treatment and follow-up. Ann Oncol 28:iv22–iv40
6. Diagnosis And Treatment Guidelines For Colorectal Cancer Working Group CSOCOC (2019) Chinese Society of Clinical Oncology (CSCO) diagnosis and treatment guidelines for colorectal cancer 2018 (English version). Chin J Cancer Res 31:117–134
7. Mirkin KA, Kulaylat AS, Hollenbeak CS, Messaris E (2018) Prognostic significance of tumor deposits in stage III colon cancer. Ann Surg Oncol 25:3179–3184
8. Wind J, Lagarde SM, Ten Kate FJ, Ubbink DT, Bemelman WA, van Lanschot JJ (2007) A systematic review on the significance of extracapsular lymph node involvement in gastrointestinal malignancies. Eur J Surg Oncol 33:401–408
9. Yamano T, Semba S, Noda M et al (2015) Prognostic significance of classified extramural tumor deposits and extracapsular lymph node invasion in T3-4 colorectal cancer: a retrospective single-center study. BMC Cancer 15:859
10. Kim CW, Kim J, Park Y et al (2019) Prognostic implications of extranodal extension in relation to colorectal cancer location. Cancer Res Treat 51:1135–1143
11. Horvat N, Carlos TRC, Clemente OB, Petkovska I, Gollub MJ (2019) MRI of rectal cancer: tumor staging, imaging techniques, and management. Radiographics 39:367–387
12. Brown G, Richards CJ, Bourne MW et al (2003) Morphologic predictors of lymph node status in rectal cancer with use of high-spatial-resolution MR imaging with histopathologic comparison. Radiology 227:371–377
13. Kim JH, Beets GL, Kim MJ, Kessels AG, Beets-Tan RG (2004) High-resolution MR imaging for nodal staging in rectal cancer: are there any criteria in addition to the size? Eur J Radiol 52:78–83
14. Koh DM, Collins DJ (2007) Diffusion-weighted MRI in the body: applications and challenges in oncology. AJR Am J Roentgenol 188:1622–1635
15. Nelson DA, Tan TT, Rabson AB, Anderson D, Degenhardt K, White E (2004) Hypoxia and defective apoptosis drive genomic instability and tumorigenesis. Genes Dev 18:2095–2107
16. Mori N, Mugikura S, Takasawa C et al (2016) Peritumoral apparent diffusion coefficients for prediction of lymphovascular invasion in clinically node-negative invasive breast cancer. Eur Radiol 26:331–339
17. Hu Y, Xie C, Yang H et al (2020) Assessment of intratumoral and peritumoral computed tomography radiomics for predicting pathological complete response to neoadjuvant chemoradiation in patients with esophageal squamous cell carcinoma. JAMA Netw Open 3:e2015927
18. Deng L, Wang QP, Yan R et al (2018) The utility of measuring the apparent diffusion coefficient for peritumoral zone in assessing infiltration depth of endometrial cancer. Cancer Imaging 18:23
19. Liu J, Li Q, Tang L, Huang Z, Lin Q (2021) Correlations of mean and minimum apparent diffusion coefficient values with the clinicopathological features in rectal cancer. Acad Radiol 28:S105–S111
20. Li H, Chen GW, Liu YS et al (2020) Assessment of histologic prognostic factors of resectable rectal cancer: comparison of diagnostic performance using various apparent diffusion coefficient parameters. Sci Rep 10:11554
21. Kim YI, Cho H, Kim CW et al (2021) Prognostic impact of extranodal extension in rectal cancer patients undergoing radical resection after preoperative chemoradiotherapy. Clin Colorectal Cancer 20:e35–e42
22. Koo TK, Li MY (2016) A guideline of selecting and reporting intraclass correlation coefficients for reliability research. J Chiropr Med 15:155–163
23. Giavarina D (2015) Understanding Bland Altman analysis. Biochem Med (Zagreb) 25:141–151
24. Youden WJ (1950) Index for rating diagnostic tests. Cancer 3:32–35
25. Curvo-Semedo L, Lambregts DM, Maas M, Beets GL, Caseiro-Alves F, Beets-Tan RG (2012) Diffusion-weighted MRI in rectal cancer: apparent diffusion coefficient as a potential noninvasive marker of tumor aggressiveness. J Magn Reson Imaging 35:1365–1371
26. Sun Y, Tong T, Cai S, Bi R, Xin C, Gu Y (2014) Apparent diffusion coefficient (ADC) value: a potential imaging biomarker that reflects the biological features of rectal cancer. PLoS One 9:e109371
27. Orel VE, Ashykhmin A, Golovko T, Rykhalskyi O, Orel VB (2021) Texture analysis of tumor and peritumoral tissues based on 18F-fluorodeoxyglucose positron emission tomography/computed tomography hybrid imaging in patients with rectal cancer. J Comput Assist Tomogr 45:820–828

28. Chen LD, Li W, Xian MF et al (2020) Preoperative prediction of tumour deposits in rectal cancer by an artificial neural network-based US radiomics model. Eur Radiol 30:1969–1979
29. Uematsu T, Kasami M, Watanabe J (2014) Is evaluation of the presence of prepectoral edema on T2-weighted with fat suppression 3 T breast MRI a simple and readily available noninvasive technique for estimation of prognosis in patients with breast cancer? Breast Cancer 21:684–692
30. Cheon H, Kim HJ, Kim TH et al (2018) Invasive breast cancer: prognostic value of peritumoral edema identified at preoperative MR imaging. Radiology 287:68–75
31. Braithwaite AC, Dale BM, Boll DT, Merkle EM (2009) Short- and midterm reproducibility of apparent diffusion coefficient measurements at 3.0-T diffusion-weighted imaging of the abdomen. Radiology 250:459–465
32. Kettunen T, Okuma H, Auvinen P et al (2020) Peritumoral ADC values in breast cancer: region of interest selection, associations with hyaluronan intensity, and prognostic significance. Eur Radiol 30:38–46

Publisher's note Springer Nature remains neutral with regard to jurisdictional claims in published maps and institutional affiliations.

Affiliations

Yi Yuan[1] · Xiao-li Chen[2] · Zhen-lin Li[3] · Guang-wen Chen[1] · Hao Liu[4] · Yi-Sha Liu[5] · Ming-hui Pang[6] · Si-yun Liu[7] · Hong Pu[1] · Hang Li[1]

[1] Department of Radiology, Sichuan Academy of Medical Sciences and Sichuan Provincial People's Hospital, 32# Second Section of First Ring Road, Qingyang District, Chengdu 610070 Sichuan, China

[2] Department of Radiology, Affiliated Cancer Hospital of Medical School, University of Electronic Science and Technology of China, Sichuan Cancer Hospital, Chengdu 610000, China

[3] Department of Radiology, West China Hospital, Sichuan University, Chengdu 610041, China

[4] Department of Oncology, Sichuan Academy of Medical Sciences and Sichuan Provincial People's Hospital, 32# Second Section of First Ring Road, Qingyang District, Chengdu 610070, Sichuan, China

[5] Department of Pathology, Sichuan Academy of Medical Sciences and Sichuan Provincial People's Hospital, 32# Second Section of First Ring Road, Qingyang District, Chengdu 610070, Sichuan, China

[6] Department of Gastrointestinal Surgery, Sichuan Academy of Medical Sciences and Sichuan Provincial People's Hospital, 32# Second Section of First Ring Road, Qingyang District, Chengdu 610070, Sichuan, China

[7] GE Healthcare (China), 1# Tongji South Road, Daxing District, Beijing 100176, China